Electronic Supplementary Information

Thermoelectrochemical Seebeck coefficient and viscosity of Co-complex electrolytes rationalized by the Einstein relation, Jones–Dole *B* coefficient, and quantum-chemical calculations

Yuki Cho,[a] Shinya Nagatsuka,[b] and Yoichi Murakami[a,c]*

[a] Department of Mechanical Engineering, School of Engineering, Tokyo Institute of Technology, 2-12-1 Ookayama, Meguro-ku, Tokyo 152-8552, Japan.

[b] Nippon Kayaku Co., Ltd., 3-31-12 Shimo, Kita-ku, Tokyo 115-8588, Japan.

[c] Laboratory for Zero-Carbon Energy, Institute of Innovative Research, Tokyo Institute of Technology, 2-12-1 Ookayama, Meguro-ku, Tokyo 152-8550, Japan.

*Corresponding Author. E-mail: murakami.y.af@m.titech.ac.jp

List of Contents

1. Methods

1.1. Sample preparations

The Co complexes #1–5 (Fig. 1 in the main text) were synthesized based on the previous literature.[S1] All the synthesized complexes were recrystallized in ethanol. The resultant purity of > 98% for all compounds was confirmed combining characterizations by NMR, liquid chromatography–mass spectrometry (LC–MS), and ion chromatography (IC). For most of them, the molecular structures were double-checked by the single crystal X-ray structure analysis. GBL (certified purity: > 99%) was purchased from TCI in Japan. The moisture, which might be present in the as-supplied GBL, was removed before use by adding an appropriate amount of molecular sieves (pore size: 4 Å; supplier: Nacalai Tesque in Japan; activated at 200 °C under vacuum for several hours before use) to the reservoir glass bottle of GBL.

The redox species, summarized in Fig. 1 of the main text, were dissolved in GBL by ultrasonication for 2–5 min depending on the concentration. The complete dissolution was checked visibly by irradiating the solution in a glass vial with a low-intensity laser beam (wavelength: 632.8 nm, power: 5–10 mW) and the absence of particulate light scattering in it. The dissolution of the solutes was indirectly supported by the fact that the concentrations used in this study were below their solubility limits in GBL, which were approximately 0.5 M at room temperature.

Because of the relatively large molecular volume of the solutes used in this study, the increase of the solution volume by the solute was correctly considered when calculating the molar concentration c. The determinations of c were carried out at room temperature controlled to 25±0.5 °C. We estimate that the certainty of c was within ±1%.

1.2. Quantum-chemical simulations

All quantum-chemical simulations were carried out using Gaussian 16® software. We used ωB97XD/6-31+G(d,p) as our main level of theory, in addition to the B3LYP/6-31+G(d,p) level of theory for the purpose of checking the former results. The reason for our choice of the former level of theory is its superiority over the latter in terms of the quantitative reliability, as has been reported by multiple papers,[S2-S4] although the latter is still one of the most popular levels of theory. Therefore, in this report, all calculations were performed at the ωB97XD/6-31+G(d,p) level of theory unless otherwise specified. Specifically, the B3LYP/6-31+G(d,p) level of theory was employed only for Fig. 4 in the main text, for which their results were quantitatively close to those obtained with the ωB97XD/6-31+G(d,p) level of theory.

1.3. Estimations of the ionic radii and volumes

The radii of the cations, r_{2+} and r_{3+} for $Co(L)_i^{2+}$ and $Co(L)_i^{3+}$, respectively, were estimated by the following method using the optimized structures obtained by the quantum-chemical simulations at the ωB97XD/6-31+G(d,p) level of theory; see Table S2 below for the atomic coordinates after the structural optimizations. First, the center-to-center distances between the cobalt atom and the hydrogen atoms on the aromatic ligands, denoted L_H, were measured using Chem3D® software. The van der Waals radius of a hydrogen atom, r_H (= 1.20 Å),[S5] was added to L_H to obtain $R_H \equiv L_H + r_H$; see Scheme S1 below. Using the values of $R_{H,i}$ obtained for all hydrogen atoms, where i is an index for the hydrogen atom on the ligand, we define the average projection area A_{ave} as

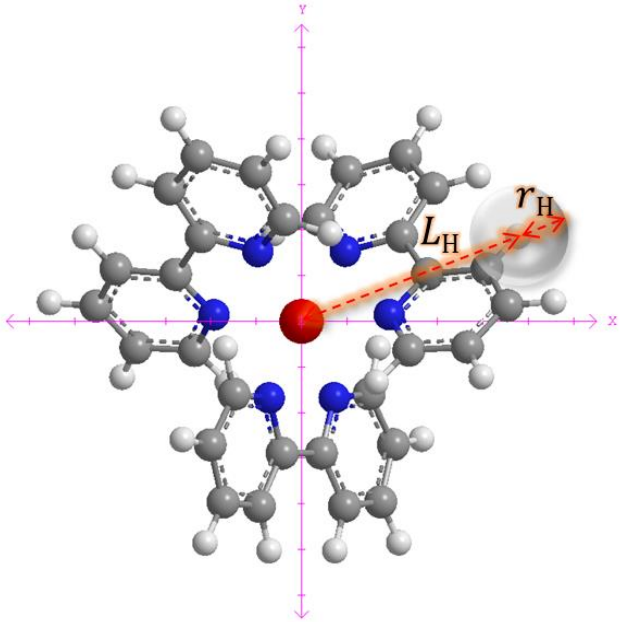

Scheme S1 The depiction of $L_H + r_H$ ($\equiv R_H$) shown on the ball-and-stick graphic of the optimized structure of $Co(bpy)_3^{2+}$ obtained at the ωB97XD/6-31+G(d,p) level of theory. The colors are assigned as follows: Red: Co; blue: N; gray: C; white: H. See Table S2 for the atomic coordinates.

$$A_{\text{ave}} \equiv \frac{1}{j}\sum_{i=1}^{j} \pi {R_{\text{H},i}}^2 , \tag{S1}$$

where j is the number of the hydrogen atoms on the polypyridine ligand. Finally, r_x (x: 2+ or 3+) was determined from the relationship $\pi {r_x}^2 = A_{\text{ave}}$.

Similarly, the radii of the anions r_{an} were estimated as follows. In this case, because the shape symmetry of the anions, especially FSI^- and $TFSI^-$, was much lower than those of the cations, we chose the geometrical center of each anion as its spatial origin. First, the distances between this origin and the centers of all fluorine atoms in the anion, denoted L_F, were measured using Chem3D® software. Then, the van der Waals radius of the fluorine atom, r_F (= 1.74 Å),[S5] was added to L_F to obtain $R_F \equiv L_F + r_F$. In a procedure similar to that used for the cations above, A_{ave} for the anion was obtained by

$$A_{\mathrm{ave}} \equiv \frac{1}{j}\sum_{i=1}^{j} \pi {R_{\mathrm{F},i}}^2 . \qquad \text{(S2)}$$

Finally, r_{an} was determined from the relationship $\pi {r_{\mathrm{an}}}^2 = A_{\mathrm{ave}}$. See Scheme S1 for the graphical depiction of the structure of $Co(bpy)_3^{2+}$.

We use A_{ave} in the estimation of these radii because the hydrodynamic drag forces exerted on a particle moving in the fluid depend fundamentally on the projection area of the particle.[S6] All radii are summarized in Table S1 below. In the previous work by Pringle and co-workers,[S7] a similar method was used to estimate the ionic radii of the polypyridine Co complexes.

Using the ionic radii obtained thereby, the partial molar volume of the redox species, $\bar{V}$, was calculated from the relationship

$$\bar{V} = \frac{4\pi}{3}({r_{2+}}^3 + {r_{3+}}^3 + 5{r_{\mathrm{an}}}^3)N_{\mathrm{A}} , \qquad \text{(S3)}$$

where N_{A} is the Avogadro constant.

1.4. Viscosity measurements

Viscosities were measured using a cone-plate rheometer (Brookfield, DV2T, USA), where the temperature was controlled by the circulation of temperature-controlled water in the sample cup. Unless otherwise specified, the viscosities were measured at 25.0 °C, as measured by the thermocouple embedded in the sample cup of the rheometer. Especially when the datasets of the viscosity presented in Fig. 3a of the main text were acquired, the room temperature was carefully controlled and maintained at 25±0.2 °C by

the room air conditioner, which was checked by a digital thermometer placed near the rheometer during the measurements to minimize the experimental errors.

1.5. Measurements of the Seebeck coefficient

The Seebeck coefficient was determined using our homebuilt non-isothermal measurement system used in our previous report.[S8] In this system, two small glass vials containing the same electrolyte liquid connected by a salt bridge (a PFA fluorocarbon resin tube filled with the same electrolyte) were mounted in the cylindrical bores of the cold and hot blocks (nickel-plated copper) with the bore diameter slightly larger than the outer diameter of the glass vial. The small gap between the bore wall and the outer wall of the glass vial was filled with an ionic liquid to achieve a good thermal contact between them during the measurements. The temperatures of these blocks were independently controlled by a Peltier unit (cold block) and an embedded rod heater (hot block) with digital-feedback temperature controllers.

The electromotive force (emf) between two electrodes, which were platinum wires immersed in the electrolyte, was measured using a Digital Multimeter (Keysight, 34465A). The actual temperature of the electrolyte in each vial was recorded with a thermocouple immersed in it, from which the temperature difference ΔT was obtained. To acquire each datapoint, a waiting time of at least 30 min was taken after the new temperature was set on the temperature controller to ensure the achievement of a steady state. Then, the emf at each temperature was obtained from the average value over 10 min. Finally, the value of *Se* was determined from the least-square linear fit to the slope of the datapoints; see Fig. S2 below for the experimental data.

1.6. Conductance measurements

The electrical conductance, or conductivity, of the electrolytes was measured by the alternating current (AC) impedance method scanned from 300 kHz to 0.4 Hz using a potentiostat–galvanostat (VersaSTAT 4, Princeton Applied Research, USA) with a potential wave amplitude of 5 mV. The conductivity was determined from the first touchdown point on the real axis of the Nyquist plot. The temperature of the sample was controlled by circulating temperature-controlled water through our custom-made electrochemical cell that had been hermetically sealed using O-rings; this experimental setup was also used in our previous report.[S8] The temperature of the sample was measured using a T-type sheath thermocouple embedded in the cell with an accuracy of ±0.1 °C. To ensure the attainment of a steady state, a waiting time of at least 30 min was imposed before each AC impedance measurement was started.

2. Summary of the calculated radii

Tables S1 summarises the calculated radii of $Co(L)_i^{2+}$ and $Co(L)_i^{3+}$ (L: ligand), denoted r_{2+} and r_{3+}, respectively, and that of the counter anion, denoted r_{an}, obtained by quantum chemical simulations at the ωB97XD/6-31+G(d,p) level of theory. See Section 1.3 above for the method of determining these ionic radii.

Table S1. Summary of the radii calculated by the quantum-chemical simulations.

	r_{2+} / Å	r_{3+} / Å	r_{cat}[a] / Å	r_{an} / Å
$Co^{II}(bpy)_3^{2+}$	6.169	—	6.089	—
$Co^{III}(bpy)_3^{3+}$	—	6.009		—
$Co^{II}(tpy)_2^{2+}$	6.292	—	6.207	—
$Co^{III}(tpy)_2^{3+}$	—	6.123		—
$Co^{II}(phen)_3^{2+}$	6.541	—	6.456	—
$Co^{III}(phen)_3^{3+}$	—	6.372		—
FSI^-	—	—	—	3.687
$TFSI^-$	—	—	—	4.359
$TFSM^-$	—	—	—	4.922

[a] $r_{cat} = (r_{2+} + r_{3+})/2$.

3. Atomic coordinates after the structural optimizations

The following Tables S2-A to S2-I summarize the atomic coordinates of all cations and anions investigated in this study after structural optimizations by the quantum-chemical calculations carried out at the ωB97XD/6-31+G(d,p) and B3LYP/6-31+G(d,p) levels of theory, which are shown in the left and right columns below, respectively.

Table S2-A. Atomic coordinates of the structure-optimized complex $Co(bpy)_3^{2+}$

	ωB97XD			**B3LYP**		
	X	Y	Z	X	Y	Z
C(1)	-1.733	-3.673	2.316	-1.645	-3.682	2.382
C(2)	-0.932	-3.767	1.183	-0.874	-3.764	1.224
C(3)	-0.429	-2.603	0.606	-0.409	-2.590	0.618
N(4)	-0.714	-1.390	1.120	-0.706	-1.373	1.135
C(5)	-1.489	-1.304	2.208	-1.453	-1.301	2.250
C(6)	-2.016	-2.419	2.845	-1.941	-2.426	2.910
C(7)	0.438	-2.601	-0.606	0.420	-2.588	-0.618
C(8)	0.944	-3.764	-1.183	0.887	-3.761	-1.224
C(9)	1.744	-3.668	-2.317	1.659	-3.676	-2.382
C(10)	2.025	-2.412	-2.845	1.951	-2.419	-2.911
C(11)	1.494	-1.300	-2.207	1.459	-1.296	-2.249
N(12)	0.720	-1.388	-1.120	0.712	-1.370	-1.135
H(13)	-2.131	-4.571	2.777	-2.010	-4.585	2.860
H(14)	-0.718	-4.740	0.758	-0.646	-4.735	0.802
H(15)	-1.686	-0.302	2.573	-1.662	-0.303	2.621
H(16)	-2.636	-2.301	3.726	-2.537	-2.314	3.809
H(17)	0.732	-4.737	-0.759	0.663	-4.733	-0.803
H(18)	2.145	-4.564	-2.778	2.026	-4.578	-2.861
H(19)	2.644	-2.293	-3.726	2.547	-2.305	-3.809
H(20)	1.689	-0.296	-2.572	1.666	-0.297	-2.620
C(21)	4.538	0.638	1.835	4.555	0.763	1.900
C(22)	4.094	1.448	0.795	4.114	1.548	0.836
C(23)	2.777	1.329	0.354	2.802	1.403	0.368
N(24)	1.933	0.438	0.909	1.956	0.505	0.929
C(25)	2.366	-0.343	1.905	2.389	-0.251	1.952
C(26)	3.659	-0.276	2.406	3.677	-0.155	2.474
C(27)	2.210	2.153	-0.750	2.250	2.202	-0.759
C(28)	2.900	3.205	-1.351	2.963	3.233	-1.385
C(29)	2.291	3.919	-2.377	2.376	3.935	-2.436
C(30)	1.006	3.571	-2.777	1.085	3.596	-2.840
C(31)	0.379	2.519	-2.124	0.434	2.565	-2.167
N(32)	0.962	1.825	-1.140	0.995	1.882	-1.155
H(33)	5.560	0.719	2.190	5.570	0.867	2.270
H(34)	4.776	2.153	0.338	4.793	2.257	0.379
H(35)	1.643	-1.044	2.310	1.673	-0.955	2.362
H(36)	3.965	-0.925	3.218	3.977	-0.787	3.303
H(37)	3.896	3.478	-1.026	3.962	3.495	-1.060
H(38)	2.816	4.740	-2.855	2.920	4.735	-2.928
H(39)	0.496	4.102	-3.572	0.589	4.115	-3.653
H(40)	-0.628	2.211	-2.391	-0.574	2.270	-2.442
C(41)	-2.301	3.911	2.380	-2.384	3.927	2.439
C(42)	-2.908	3.195	1.353	-2.970	3.224	1.388
C(43)	-2.214	2.146	0.752	-2.254	2.195	0.761
N(44)	-0.966	1.822	1.141	-0.997	1.878	1.157
C(45)	-0.384	2.517	2.126	-0.438	2.563	2.169
C(46)	-1.015	3.566	2.780	-1.092	3.591	2.843
C(47)	-2.780	1.321	-0.353	-2.803	1.395	-0.366
C(48)	-4.096	1.436	-0.794	-4.116	1.536	-0.834
C(49)	-4.538	0.625	-1.835	-4.555	0.750	-1.898
C(50)	-3.656	-0.285	-2.406	-3.674	-0.165	-2.473

C(51)	-2.363	-0.349	-1.905	-2.386	-0.257	-1.950
N(52)	-1.933	0.433	-0.908	-1.955	0.500	-0.928
H(53)	-2.829	4.729	2.858	-2.930	4.726	2.931
H(54)	-3.905	3.465	1.029	-3.969	3.484	1.062
H(55)	0.623	2.212	2.393	0.570	2.271	2.443
H(56)	-0.507	4.098	3.575	-0.598	4.112	3.656
H(57)	-4.781	2.139	-0.337	-4.796	2.243	-0.376
H(58)	-5.560	0.704	-2.190	-5.570	0.851	-2.268
H(59)	-3.960	-0.935	-3.218	-3.972	-0.797	-3.302
H(60)	-1.638	-1.048	-2.310	-1.668	-0.959	-2.361
Co(61)	0.000	0.289	0.000	0.001	0.337	0.000

Table S2-B. Atomic coordinates of the structure-optimized complex $Co(bpy)_3^{3+}$

ωB97XD				**B3LYP**		
	X	Y	Z	X	Y	Z
C(1)	2.992	-2.847	2.283	3.030	-2.867	2.284
C(2)	3.371	-2.076	1.188	3.401	-2.091	1.186
C(3)	2.432	-1.253	0.578	2.458	-1.260	0.578
N(4)	1.156	-1.187	1.030	1.178	-1.194	1.041
C(5)	0.791	-1.934	2.085	0.822	-1.946	2.102
C(6)	1.680	-2.774	2.739	1.717	-2.791	2.751
C(7)	2.708	-0.383	-0.580	2.734	-0.395	-0.580
C(8)	3.950	-0.252	-1.189	3.984	-0.262	-1.188
C(9)	4.087	0.597	-2.284	4.130	0.586	-2.286
C(10)	2.973	1.293	-2.741	3.015	1.283	-2.752
C(11)	1.762	1.119	-2.088	1.795	1.112	-2.103
N(12)	1.629	0.299	-1.033	1.651	0.293	-1.042
C(13)	0.965	4.011	2.287	0.968	4.057	2.285
C(14)	0.110	3.954	1.191	0.110	3.991	1.187
C(15)	-0.131	2.730	0.579	-0.138	2.758	0.579
N(16)	0.450	1.592	1.030	0.445	1.617	1.041
C(17)	1.277	1.649	2.087	1.274	1.684	2.102
C(18)	1.557	2.838	2.743	1.558	2.882	2.752
C(19)	-1.020	2.535	-0.581	-1.025	2.565	-0.579
C(20)	-1.752	3.547	-1.192	-1.765	3.581	-1.187
C(21)	-2.553	3.241	-2.289	-2.572	3.283	-2.286
C(22)	-2.600	1.928	-2.745	-2.618	1.969	-2.752
C(23)	-1.848	0.965	-2.089	-1.860	0.999	-2.103
N(24)	-1.073	1.259	-1.033	-1.079	1.284	-1.042
C(25)	-3.958	-1.162	2.289	-3.998	-1.189	2.286
C(26)	-3.483	-1.876	1.193	-3.512	-1.899	1.188
C(27)	-2.301	-1.477	0.581	-2.320	-1.498	0.580
N(28)	-1.604	-0.406	1.032	-1.623	-0.422	1.042
C(29)	-2.064	0.284	2.088	-2.095	0.263	2.103
C(30)	-3.236	-0.064	2.744	-3.275	-0.090	2.752
C(31)	-1.688	-2.152	-0.578	-1.709	-2.170	-0.578
C(32)	-2.200	-3.291	-1.188	-2.219	-3.320	-1.186
C(33)	-1.535	-3.835	-2.283	-1.558	-3.870	-2.284
C(34)	-0.373	-3.223	-2.739	-0.397	-3.253	-2.751
C(35)	0.086	-2.089	-2.086	0.065	-2.111	-2.102
N(36)	-0.556	-1.561	-1.031	-0.572	-1.577	-1.041
Co(37)	0.000	-0.001	-0.001	0.000	0.000	0.000
H(38)	3.713	-3.496	2.770	3.754	-3.518	2.765
H(39)	4.388	-2.124	0.820	4.416	-2.139	0.810
H(40)	-0.236	-1.849	2.415	-0.202	-1.862	2.441

H(41)	1.343	-3.356	3.588	1.383	-3.373	3.603
H(42)	4.809	-0.800	-0.821	4.840	-0.810	-0.812
H(43)	5.050	0.710	-2.771	5.096	0.698	-2.767
H(44)	3.033	1.962	-3.591	3.079	1.951	-3.604
H(45)	0.874	1.642	-2.419	0.912	1.636	-2.441
H(46)	1.164	4.959	2.777	1.169	5.009	2.766
H(47)	-0.357	4.859	0.823	-0.356	4.894	0.811
H(48)	1.716	0.717	2.417	1.713	0.755	2.441
H(49)	2.228	2.836	3.595	2.228	2.884	3.604
H(50)	-1.706	4.564	-0.824	-1.719	4.596	-0.811
H(51)	-3.130	4.019	-2.777	-3.153	4.064	-2.766
H(52)	-3.209	1.647	-3.596	-3.229	1.691	-3.604
H(53)	-1.857	-0.065	-2.420	-1.872	-0.028	-2.442
H(54)	-4.879	-1.461	2.778	-4.923	-1.490	2.767
H(55)	-4.035	-2.732	0.826	-4.061	-2.754	0.812
H(56)	-1.474	1.129	2.417	-1.510	1.107	2.441
H(57)	-3.568	0.519	3.594	-3.612	0.491	3.604
H(58)	-3.105	-3.759	-0.819	-3.121	-3.786	-0.809
H(59)	-1.921	-4.725	-2.770	-1.944	-4.764	-2.764
H(60)	0.176	-3.611	-3.589	0.149	-3.643	-3.603
H(61)	0.984	-1.584	-2.417	0.960	-1.608	-2.441

Table S2-C. Atomic coordinates of the structure-optimized complex $Co(tpy)_2^{2+}$

ωB97XD				**B3LYP**		
	X	Y	Z	X	Y	Z
Co(1)	0.000	0.000	0.000	0.000	0.000	0.000
C(2)	-2.701	-1.173	-0.089	-2.720	-1.178	-0.090
C(3)	-2.706	1.162	0.073	-2.725	1.168	0.072
C(4)	-4.094	-1.212	-0.096	-4.120	-1.213	-0.097
C(5)	-4.099	1.196	0.071	-4.124	1.199	0.070
C(6)	-4.790	-0.009	-0.014	-4.819	-0.008	-0.016
H(7)	-4.636	-2.148	-0.162	-4.661	-2.149	-0.163
H(8)	-4.645	2.129	0.134	-4.669	2.133	0.133
H(9)	-5.874	-0.012	-0.018	-5.904	-0.010	-0.019
C(10)	0.394	-3.096	-0.215	0.357	-3.147	-0.216
C(11)	-1.804	-2.362	-0.170	-1.836	-2.373	-0.170
C(12)	0.005	-4.426	-0.309	-0.055	-4.475	-0.309
H(13)	1.443	-2.816	-0.192	1.412	-2.891	-0.195
C(14)	-2.272	-3.669	-0.263	-2.324	-3.680	-0.262
C(15)	-1.355	-4.714	-0.333	-1.423	-4.743	-0.332
H(16)	0.750	-5.211	-0.363	0.680	-5.271	-0.362
H(17)	-3.334	-3.882	-0.281	-3.389	-3.876	-0.278
H(18)	-1.702	-5.738	-0.406	-1.787	-5.763	-0.404
C(19)	0.381	3.098	0.217	0.345	3.148	0.219
C(20)	-1.814	2.355	0.158	-1.846	2.367	0.158
C(21)	-0.015	4.426	0.309	-0.072	4.475	0.309
H(22)	1.431	2.822	0.201	1.401	2.895	0.204
C(23)	-2.289	3.660	0.248	-2.338	3.672	0.246
C(24)	-1.376	4.708	0.324	-1.441	4.738	0.323
H(25)	0.727	5.214	0.366	0.659	5.273	0.367
H(26)	-3.351	3.869	0.260	-3.404	3.865	0.256
H(27)	-1.727	5.732	0.395	-1.809	5.757	0.392
N(28)	-0.491	2.088	0.144	-0.511	2.118	0.145
N(29)	-2.056	-0.004	-0.006	-2.068	-0.004	-0.007
N(30)	-0.482	-2.090	-0.147	-0.503	-2.120	-0.148

C(31)	-0.397	-0.217	3.096	-0.361	-0.218	3.146
C(32)	1.802	-0.160	2.364	1.834	-0.160	2.376
C(33)	-0.008	-0.309	4.426	0.050	-0.309	4.475
H(34)	-1.446	-0.200	2.815	-1.415	-0.202	2.889
C(35)	2.269	-0.251	3.672	2.320	-0.250	3.684
C(36)	1.351	-0.326	4.715	1.417	-0.325	4.745
H(37)	-0.754	-0.366	5.210	-0.686	-0.365	5.270
H(38)	3.331	-0.264	3.886	3.385	-0.261	3.881
H(39)	1.697	-0.397	5.741	1.780	-0.395	5.766
C(40)	2.700	-0.075	1.176	2.719	-0.076	1.182
C(41)	2.707	0.087	-1.159	2.726	0.086	-1.164
C(42)	4.093	-0.075	1.217	4.118	-0.076	1.219
C(43)	4.100	0.092	-1.191	4.126	0.091	-1.193
C(44)	4.790	0.010	0.015	4.818	0.008	0.015
H(45)	4.634	-0.138	2.153	4.659	-0.140	2.156
H(46)	4.647	0.158	-2.124	4.672	0.156	-2.126
H(47)	5.874	0.012	0.019	5.904	0.010	0.019
C(48)	1.816	0.168	-2.353	1.848	0.167	-2.364
C(49)	-0.378	0.215	-3.098	-0.341	0.217	-3.148
C(50)	2.292	0.260	-3.657	2.342	0.258	-3.669
C(51)	0.018	0.309	-4.426	0.077	0.309	-4.475
H(52)	-1.429	0.194	-2.824	-1.397	0.197	-2.898
C(53)	1.380	0.331	-4.707	1.446	0.330	-4.736
H(54)	3.355	0.277	-3.865	3.408	0.273	-3.860
H(55)	-0.722	0.362	-5.215	-0.653	0.363	-5.274
H(56)	1.732	0.403	-5.730	1.816	0.401	-5.754
N(57)	0.480	-0.144	2.091	0.500	-0.145	2.120
N(58)	2.056	0.004	0.006	2.068	0.004	0.007
N(59)	0.493	0.146	-2.088	0.513	0.147	-2.117

Table S2-D. Atomic coordinates of the structure-optimized complex $Co(tpy)_2^{3+}$

ωB97XD				**B3LYP**		
	X	Y	Z	X	Y	Z
Co(1)	0.000	0.000	0.000	0.000	0.000	0.000
C(2)	-2.504	1.096	0.471	-2.526	1.101	0.473
C(3)	-2.515	-1.090	-0.427	-2.536	-1.095	-0.430
C(4)	-3.894	1.127	0.495	-3.923	1.128	0.495
C(5)	-3.905	-1.117	-0.426	-3.934	-1.119	-0.429
C(6)	-4.589	0.005	0.040	-4.621	0.005	0.039
H(7)	-4.433	1.995	0.856	-4.462	1.997	0.856
H(8)	-4.452	-1.984	-0.778	-4.480	-1.987	-0.781
H(9)	-5.674	0.007	0.050	-5.707	0.006	0.048
C(10)	0.705	2.667	1.090	0.675	2.705	1.105
C(11)	-1.557	2.147	0.894	-1.589	2.156	0.898
C(12)	0.410	3.922	1.609	0.362	3.961	1.624
H(13)	1.732	2.349	0.952	1.706	2.402	0.972
C(14)	-1.920	3.383	1.405	-1.965	3.396	1.411
C(15)	-0.921	4.286	1.769	-0.977	4.313	1.780
H(16)	1.216	4.594	1.879	1.162	4.642	1.897
H(17)	-2.964	3.647	1.522	-3.013	3.648	1.523
H(18)	-1.185	5.259	2.171	-1.253	5.283	2.181
C(19)	0.679	-2.668	-1.103	0.650	-2.706	-1.116
C(20)	-1.577	-2.143	-0.868	-1.609	-2.152	-0.872
C(21)	0.372	-3.922	-1.616	0.326	-3.962	-1.630
H(22)	1.709	-2.353	-0.982	1.684	-2.406	-1.001

C(23)	-1.952	-3.378	-1.372	-1.996	-3.391	-1.378
C(24)	-0.963	-4.283	-1.753	-1.017	-4.311	-1.763
H(25)	1.171	-4.597	-1.900	1.119	-4.644	-1.916
H(26)	-2.999	-3.640	-1.471	-3.047	-3.641	-1.473
H(27)	-1.235	-5.255	-2.150	-1.302	-5.280	-2.160
N(28)	-0.267	-1.796	-0.736	-0.287	-1.818	-0.744
N(29)	-1.872	0.002	0.016	-1.888	0.002	0.016
N(30)	-0.250	1.797	0.740	-0.270	1.819	0.749
C(31)	-0.714	1.098	-2.662	-0.684	1.112	-2.700
C(32)	1.550	0.879	-2.158	1.582	0.883	-2.167
C(33)	-0.422	1.613	-3.919	-0.376	1.628	-3.958
H(34)	-1.739	0.969	-2.336	-1.714	0.988	-2.390
C(35)	1.909	1.386	-3.397	1.953	1.393	-3.410
C(36)	0.908	1.760	-4.293	0.962	1.771	-4.320
H(37)	-1.230	1.891	-4.585	-1.178	1.908	-4.633
H(38)	2.952	1.493	-3.669	3.001	1.495	-3.670
H(39)	1.168	2.159	-5.267	1.235	2.169	-5.292
C(40)	2.500	0.446	-1.115	2.523	0.449	-1.120
C(41)	2.518	-0.452	1.071	2.540	-0.454	1.077
C(42)	3.890	0.456	-1.156	3.920	0.458	-1.157
C(43)	3.908	-0.466	1.089	3.938	-0.466	1.091
C(44)	4.589	-0.006	-0.040	4.621	-0.005	-0.039
H(45)	4.426	0.811	-2.028	4.455	0.814	-2.029
H(46)	4.458	-0.822	1.951	4.487	-0.824	1.954
H(47)	5.674	-0.007	-0.049	5.707	-0.006	-0.048
C(48)	1.584	-0.883	2.131	1.616	-0.887	2.140
C(49)	-0.671	-1.095	2.673	-0.641	-1.110	2.711
C(50)	1.963	-1.391	3.363	2.007	-1.397	3.377
C(51)	-0.359	-1.612	3.925	-0.313	-1.627	3.964
H(52)	-1.701	-0.964	2.365	-1.676	-0.985	2.418
C(53)	0.976	-1.762	4.276	1.031	-1.773	4.303
H(54)	3.011	-1.501	3.617	3.059	-1.502	3.619
H(55)	-1.156	-1.888	4.605	-1.103	-1.906	4.652
H(56)	1.252	-2.162	5.246	1.320	-2.172	5.271
N(57)	0.244	0.738	-1.799	0.264	0.747	-1.821
N(58)	1.872	-0.002	-0.016	1.888	-0.002	-0.016
N(59)	0.273	-0.739	1.794	0.293	-0.747	1.816

Table S2-E. Atomic coordinates of the structure-optimized complex $Co(phen)_3^{2+}$

ωB97XD				**B3LYP**		
	X	Y	Z	X	Y	Z
C(1)	1.281	-3.206	2.820	1.330	-3.217	2.849
C(2)	2.549	-3.491	2.365	2.601	-3.505	2.388
C(3)	3.068	-2.785	1.259	3.114	-2.803	1.272
C(4)	2.244	-1.809	0.672	2.278	-1.823	0.677
C(5)	0.535	-2.210	2.170	0.576	-2.225	2.196
C(6)	4.381	-3.018	0.722	4.424	-3.038	0.732
C(7)	2.720	-1.064	-0.467	2.751	-1.086	-0.469
C(8)	4.012	-1.310	-0.967	4.052	-1.338	-0.974
C(9)	4.834	-2.310	-0.342	4.875	-2.332	-0.345
C(10)	4.433	-0.547	-2.078	4.473	-0.583	-2.094
H(11)	5.423	-0.705	-2.495	5.463	-0.745	-2.511
C(12)	3.582	0.391	-2.619	3.619	0.354	-2.644
C(13)	2.310	0.561	-2.053	2.345	0.532	-2.076
H(14)	5.006	-3.774	1.187	5.052	-3.790	1.200

H(15)	0.853	-3.732	3.665	0.908	-3.738	3.701
H(16)	3.153	-4.254	2.848	3.209	-4.263	2.872
H(17)	-0.467	-1.959	2.503	-0.424	-1.978	2.538
H(18)	5.828	-2.489	-0.741	5.868	-2.515	-0.744
H(19)	3.876	0.994	-3.470	3.912	0.950	-3.501
H(20)	1.614	1.291	-2.456	1.653	1.260	-2.488
N(21)	1.887	-0.144	-1.013	1.916	-0.164	-1.024
N(22)	0.999	-1.528	1.133	1.030	-1.543	1.145
C(23)	1.961	2.808	2.847	1.947	2.855	2.872
C(24)	1.606	4.033	2.326	1.594	4.083	2.343
C(25)	0.805	4.089	1.166	0.799	4.135	1.175
C(26)	0.406	2.866	0.596	0.402	2.901	0.599
C(27)	1.511	1.642	2.210	1.502	1.684	2.233
C(28)	0.386	5.323	0.557	0.384	5.367	0.563
C(29)	-0.406	2.866	-0.596	-0.402	2.901	-0.599
C(30)	-0.805	4.089	-1.166	-0.800	4.135	-1.175
C(31)	-0.387	5.323	-0.557	-0.385	5.367	-0.563
C(32)	-1.606	4.032	-2.326	-1.594	4.082	-2.343
H(33)	-1.937	4.953	-2.798	-1.920	5.005	-2.815
C(34)	-1.962	2.808	-2.847	-1.948	2.855	-2.872
C(35)	-1.511	1.642	-2.210	-1.503	1.684	-2.233
H(36)	0.701	6.258	1.009	0.695	6.303	1.017
H(37)	2.578	2.731	3.735	2.557	2.781	3.766
H(38)	1.936	4.953	2.798	1.919	5.005	2.815
H(39)	1.771	0.661	2.595	1.764	0.707	2.628
H(40)	-0.702	6.258	-1.009	-0.697	6.303	-1.017
H(41)	-2.578	2.731	-3.735	-2.557	2.780	-3.766
H(42)	-1.771	0.660	-2.595	-1.764	0.707	-2.628
N(43)	-0.753	1.665	-1.122	-0.751	1.698	-1.133
N(44)	0.753	1.665	1.122	0.751	1.698	1.133
C(45)	-3.582	0.391	2.619	-3.619	0.354	2.644
C(46)	-4.433	-0.548	2.078	-4.473	-0.583	2.094
C(47)	-4.012	-1.310	0.967	-4.052	-1.338	0.974
C(48)	-2.720	-1.064	0.467	-2.751	-1.086	0.469
C(49)	-2.310	0.561	2.053	-2.345	0.531	2.076
C(50)	-4.834	-2.310	0.342	-4.875	-2.333	0.345
C(51)	-2.243	-1.809	-0.672	-2.278	-1.823	-0.677
C(52)	-3.068	-2.786	-1.259	-3.113	-2.803	-1.272
C(53)	-4.381	-3.019	-0.722	-4.423	-3.038	-0.732
C(54)	-2.549	-3.492	-2.365	-2.601	-3.505	-2.388
H(55)	-3.152	-4.255	-2.848	-3.208	-4.264	-2.872
C(56)	-1.280	-3.206	-2.820	-1.330	-3.217	-2.849
C(57)	-0.535	-2.211	-2.170	-0.576	-2.225	-2.196
H(58)	-5.827	-2.490	0.741	-5.868	-2.515	0.744
H(59)	-3.877	0.994	3.470	-3.912	0.950	3.501
H(60)	-5.422	-0.705	2.495	-5.463	-0.746	2.511
H(61)	-1.614	1.291	2.456	-1.653	1.259	2.488
H(62)	-5.006	-3.775	-1.187	-5.051	-3.790	-1.200
H(63)	-0.853	-3.732	-3.665	-0.907	-3.738	-3.701
H(64)	0.468	-1.959	-2.503	0.424	-1.978	-2.538
N(65)	-1.887	-0.144	1.013	-1.916	-0.165	1.024
N(66)	-0.999	-1.528	-1.133	-1.030	-1.543	-1.145
Co(67)	0.000	-0.002	0.000	0.000	-0.003	0.000

Table S2-F. Atomic coordinates of the structure-optimized complex $Co(phen)_3^{3+}$

	ωB97XD			**B3LYP**		
	X	Y	Z	X	Y	Z
C(1)	1.505	-2.920	2.738	1.543	-2.936	2.754
C(2)	2.787	-3.090	2.256	2.827	-3.108	2.265
C(3)	3.208	-2.346	1.131	3.245	-2.362	1.137
C(4)	2.274	-1.466	0.567	2.302	-1.475	0.569
C(5)	0.639	-2.012	2.111	0.671	-2.026	2.129
C(6)	4.516	-2.433	0.539	4.552	-2.449	0.543
C(7)	2.618	-0.681	-0.568	2.644	-0.695	-0.570
C(8)	3.898	-0.774	-1.134	3.935	-0.788	-1.139
C(9)	4.847	-1.680	-0.543	4.883	-1.692	-0.546
C(10)	4.160	0.039	-2.258	4.200	0.024	-2.268
H(11)	5.134	0.010	-2.737	5.176	-0.006	-2.743
C(12)	3.167	0.869	-2.739	3.204	0.853	-2.756
C(13)	1.914	0.893	-2.111	1.944	0.878	-2.130
H(14)	5.240	-3.114	0.974	5.277	-3.129	0.978
H(15)	1.152	-3.476	3.598	1.192	-3.491	3.617
H(16)	3.468	-3.788	2.733	3.510	-3.806	2.740
H(17)	-0.368	-1.861	2.480	-0.333	-1.878	2.506
H(18)	5.838	-1.753	-0.980	5.875	-1.765	-0.982
H(19)	3.337	1.506	-3.599	3.374	1.487	-3.619
H(20)	1.122	1.534	-2.480	1.155	1.517	-2.506
C(21)	1.776	2.764	2.738	1.772	2.804	2.754
C(22)	1.282	3.959	2.256	1.279	4.002	2.265
C(23)	0.427	3.952	1.132	0.424	3.991	1.137
C(24)	0.133	2.703	0.567	0.127	2.731	0.569
C(25)	1.424	1.561	2.111	1.419	1.594	2.129
C(26)	-0.153	5.128	0.540	-0.154	5.166	0.544
C(27)	-0.720	2.608	-0.568	-0.720	2.637	-0.570
C(28)	-1.280	3.762	-1.133	-1.285	3.803	-1.138
C(29)	-0.972	5.037	-0.542	-0.976	5.076	-0.545
C(30)	-2.116	3.582	-2.257	-2.121	3.626	-2.266
H(31)	-2.579	4.440	-2.735	-2.582	4.487	-2.742
C(32)	-2.337	2.307	-2.738	-2.341	2.349	-2.755
C(33)	-1.730	1.210	-2.110	-1.734	1.246	-2.129
H(34)	0.073	6.096	0.976	0.072	6.135	0.979
H(35)	2.435	2.737	3.598	2.428	2.778	3.617
H(36)	1.545	4.898	2.734	1.542	4.943	2.740
H(37)	1.798	0.613	2.480	1.793	0.650	2.506
H(38)	-1.405	5.932	-0.977	-1.408	5.971	-0.981
H(39)	-2.974	2.136	-3.598	-2.976	2.180	-3.618
H(40)	-1.888	0.204	-2.479	-1.893	0.243	-2.505
C(41)	-3.279	0.158	2.739	-3.313	0.133	2.756
C(42)	-4.067	-0.868	2.259	-4.104	-0.893	2.268
C(43)	-3.634	-1.605	1.134	-3.668	-1.628	1.140
C(44)	-2.406	-1.236	0.569	-2.429	-1.255	0.571
C(45)	-2.061	0.454	2.111	-2.090	0.433	2.130
C(46)	-4.363	-2.696	0.543	-4.396	-2.718	0.547
C(47)	-1.899	-1.927	-0.567	-1.924	-1.943	-0.568
C(48)	-2.619	-2.989	-1.131	-2.651	-3.014	-1.136
C(49)	-3.877	-3.359	-0.539	-3.907	-3.384	-0.542
C(50)	-2.045	-3.623	-2.256	-2.080	-3.651	-2.264
H(51)	-2.558	-4.452	-2.734	-2.595	-4.481	-2.739
C(52)	-0.831	-3.177	-2.738	-0.865	-3.202	-2.754

C(53)	-0.184	-2.103	-2.110	-0.213	-2.124	-2.129
H(54)	-5.315	-2.983	0.980	-5.348	-3.006	0.983
H(55)	-3.584	0.742	3.600	-3.618	0.715	3.619
H(56)	-5.012	-1.110	2.737	-5.050	-1.136	2.743
H(57)	-1.428	1.252	2.480	-1.459	1.228	2.506
H(58)	-4.435	-4.181	-0.975	-4.467	-4.206	-0.978
H(59)	-0.365	-3.643	-3.598	-0.401	-3.668	-3.617
H(60)	0.766	-1.737	-2.480	0.735	-1.760	-2.506
Co(61)	0.000	0.000	0.000	0.000	0.000	0.000
N(62)	1.642	0.133	-1.054	1.665	0.121	-1.064
N(63)	1.014	-1.297	1.054	1.039	-1.308	1.063
N(64)	-0.936	1.355	-1.053	-0.938	1.382	-1.063
N(65)	0.617	1.528	1.053	0.614	1.554	1.064
N(66)	-1.630	-0.229	1.054	-1.652	-0.245	1.064
N(67)	-0.706	-1.488	-1.053	-0.728	-1.503	-1.063

Table S2-G. Atomic coordinates of the structure-optimized complex $TFSI^-$

ωB97XD				**B3LYP**		
	X	Y	Z	X	Y	Z
N(1)	0.000	0.000	0.000	0.000	0.000	0.000
S(2)	0.000	1.602	0.000	0.000	1.623	0.000
S(3)	-1.293	-0.930	0.000	-1.335	-0.893	0.000
O(4)	-1.177	2.260	-0.553	-0.734	2.273	-1.097
O(5)	0.599	2.143	1.213	-0.078	2.224	1.340
O(6)	-2.494	-0.343	0.578	-2.572	-0.200	0.391
O(7)	-0.891	-2.273	0.395	-1.026	-2.207	0.576
C(8)	1.321	1.852	-1.295	1.817	1.798	-0.481
C(9)	-1.714	-1.145	-1.810	-1.603	-1.305	-1.828
F(10)	2.484	1.299	-0.939	2.641	1.233	0.416
F(11)	1.526	3.168	-1.466	2.115	3.115	-0.544
F(12)	0.955	1.338	-2.472	2.072	1.263	-1.687
F(13)	-0.677	-1.653	-2.488	-0.522	-1.912	-2.356
F(14)	-2.060	0.008	-2.382	-1.863	-0.209	-2.556
F(15)	-2.743	-1.997	-1.935	-2.651	-2.148	-1.955

Table S2-H. Atomic coordinates of the structure-optimized complex FSI^-

ωB97XD				**B3LYP**		
	X	Y	Z	X	Y	Z
N(1)	0.000	0.000	0.000	0.000	0.000	0.000
S(2)	0.000	1.595	0.000	0.000	1.611	0.000
S(3)	-1.347	-0.855	0.000	-1.363	-0.860	0.000
O(4)	-1.038	2.240	0.778	-1.041	2.273	0.782
O(5)	1.368	2.051	0.114	1.383	2.062	0.107
O(6)	-1.000	-2.254	-0.117	-1.006	-2.269	-0.109
O(7)	-2.448	-0.323	-0.776	-2.478	-0.332	-0.781
F(8)	-0.397	1.957	-1.548	-0.403	1.980	-1.572
F(9)	-1.863	-0.716	1.549	-1.889	-0.717	1.573

Table S2-I. Atomic coordinates of the structure-optimized complex $TFSM^-$

	ωB97XD			**B3LYP**		
	X	Y	Z	X	Y	Z
C(1)	0.000	0.000	0.000	0.000	0.000	0.000
S(2)	0.000	1.729	0.000	0.000	1.744	0.000
S(3)	-1.539	-0.821	0.000	-1.552	-0.833	0.000
S(4)	1.494	-0.878	-0.020	1.510	-0.883	0.004
O(5)	-2.450	-0.292	1.000	-2.472	-0.298	1.007
O(6)	1.380	-2.178	0.615	1.385	-2.201	0.626
O(7)	-1.345	2.174	-0.342	-1.354	2.192	-0.354
C(8)	1.809	-1.281	-1.823	1.889	-1.280	-1.814
C(9)	-2.363	-0.385	-1.662	-2.400	-0.410	-1.681
C(10)	0.195	2.251	1.791	0.184	2.298	1.810
O(11)	-1.313	-2.252	-0.112	-1.319	-2.275	-0.110
O(12)	2.580	0.021	0.333	2.592	0.024	0.396
O(13)	1.158	2.299	-0.664	1.172	2.318	-0.663
F(14)	-0.783	1.754	2.544	-0.791	1.789	2.574
F(15)	0.137	3.589	1.849	0.099	3.643	1.849
F(16)	1.362	1.858	2.293	1.365	1.935	2.325
F(17)	0.855	-2.072	-2.315	0.944	-2.069	-2.348
F(18)	1.867	-0.174	-2.560	1.978	-0.164	-2.550
F(19)	2.981	-1.919	-1.924	3.068	-1.927	-1.879
F(20)	-1.468	0.019	-2.565	-1.504	-0.046	-2.613
F(21)	-3.297	0.546	-1.525	-3.318	0.550	-1.557
F(22)	-2.952	-1.494	-2.127	-3.023	-1.524	-2.115

4. Calculated entropies for $Fe(bpy)_3^{2+/3+}$ and $Cr(bpy)_3^{2+/3+}$

As mentioned in the Introduction of the main text, the Co complexes are known to show higher values of *Se* owing to the $(t_{2g})^6 \rightarrow (t_{2g})^5(e_g)^2$ transition upon oxidation of $Co(L)_i^{2+}$ to $Co(L)_i^{3+}$, compared with similar complexes consisting of other transition-metal atoms, such as Fe and Cr, as experimentally obtained and reported previously.[S9] To check if this tendency can be reproduced within the present quantum-chemical simulations, we calculated the entropies (S_{vib} and S_{ele}) of $Fe(bpy)_2^{2+/3+}$ and $Cr(bpy)_2^{2+/3+}$ and compared them with those of $Co(bpy)_2^{2+/3+}$ used in this study. The results are shown in Fig. S1. From the results, the present quantum-chemical simulations have been confirmed to be

able to reproduce the superiority of the Co-complex over other transition-metal complexes for generating a large inner-shell entropy difference between the reduced and oxidized forms.

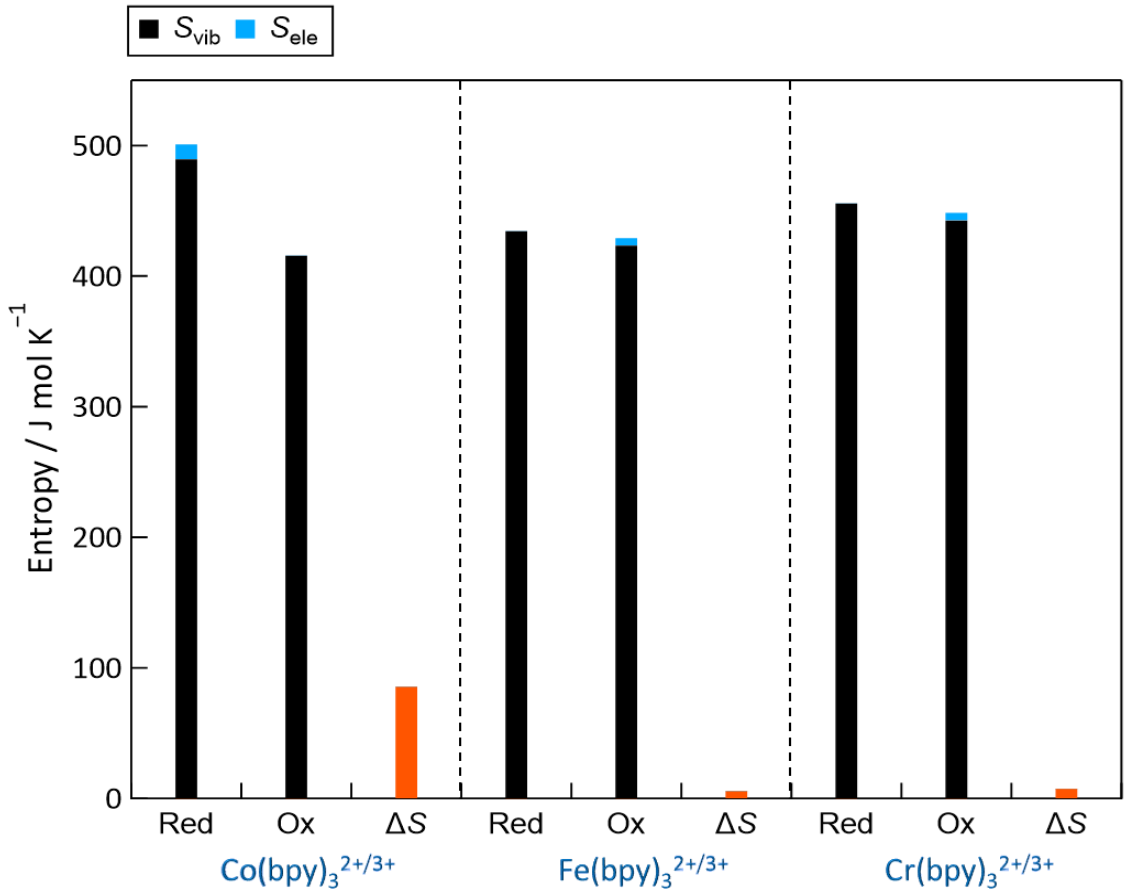

Fig. S1 Inner-shell entropies, S_{vib} and S_{ele}, for the reduced (red) and oxidized (ox) forms and their difference (ΔS) for the Co(bpy)$_3^{2+/3+}$, Fe(bpy)$_3^{2+/3+}$, and Cr(bpy)$_3^{2+/3+}$ cations, quantum-chemically calculated at the ωB97XD/6-31+G(d,p) level of theory. The magnitude of ΔS for the Co complex is much larger than those for the Fe and Cr complexes (bars in orange).

5. Data from the *Se* measurements

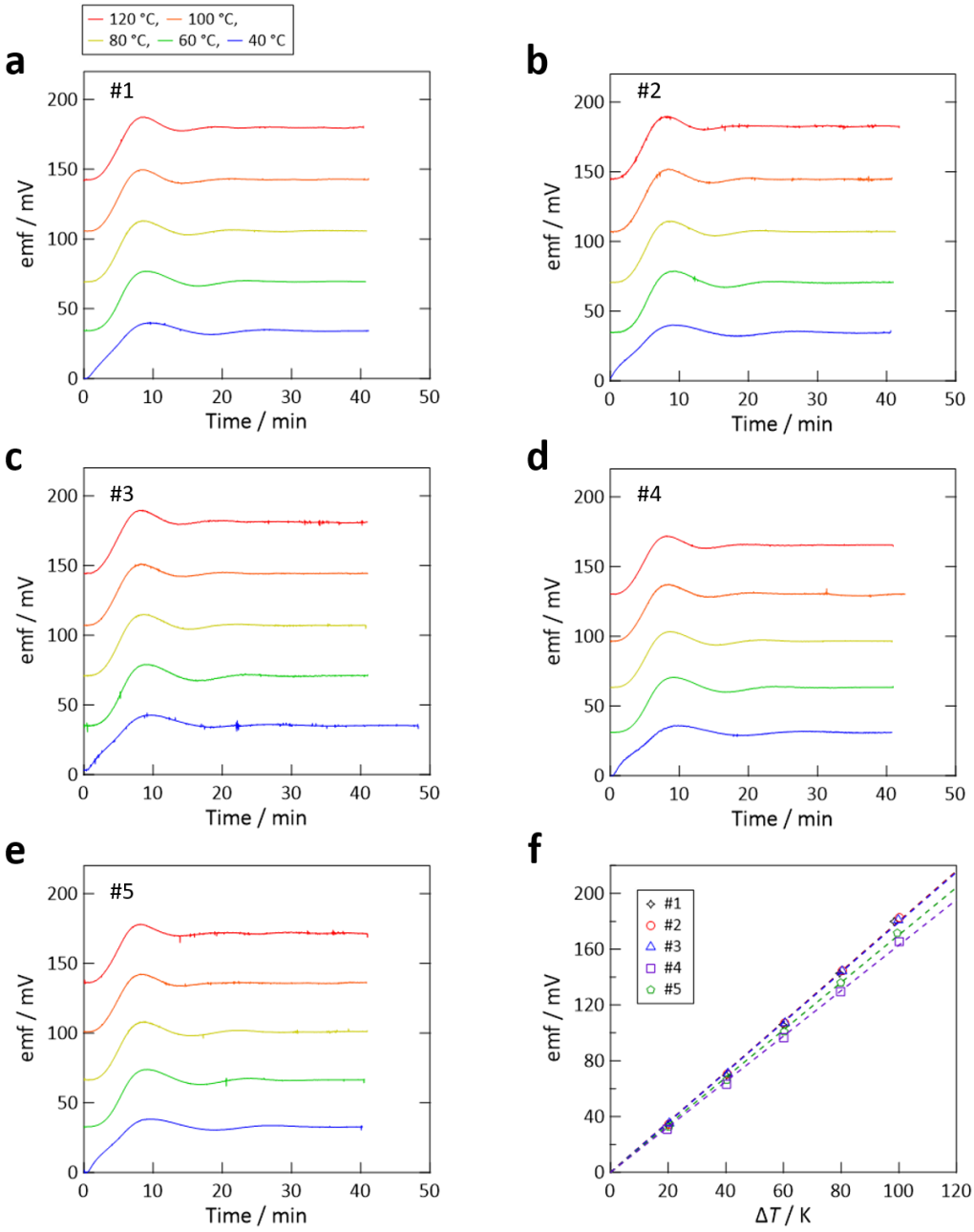

Fig. S2 (a) to (e): Raw data of the emf measurements for the GBL solutions of the redox couples #1 to 5 (concentration: 0.01 M). See Section 1.5 above for the measurement method. In each panel, the temporal changes of the measured emf were displayed for different hot-side temperatures, while the cold-side temperature was fixed at 20 °C. The average value over the last 10 min was adopted as the value of the emf for that condition. (f) Relationships between the emf and ΔT (= $T_{hot} - T_{cold}$) for the five redox couples, from which the *Se* values were determined from the slope of the least-squire linear fits to the datapoints with the constraint of passing the origin. See Table 1 of the main text for the summary of the values of *Se*.

6. Fitting parameters for the Casteel–Amis equation

The parameters resulted from the fittings demonstrated in Fig. 5a in the main text are summarized in Table S3 below.

Table S3. Parameters resulted from the fittings to the data shown in Fig. 5a in the main text.

T / °C	c_p / M	σ_p / mS cm^{-1}	α	β
45	0.189	14.9	0.679	0.332
35	0.179	12.6	0.740	0.282
25	0.167	10.4	0.805	0.229
15	0.157	8.42	0.835	0.208

7. Derivation of Equation 13

The general form of the Nernst–Einstein equation is[S10,S11]

$$\Lambda_{\mathrm{NE}} = \frac{F^2}{RT}(v_+ {z_+}^2 D_+ + v_- {z_-}^2 D_-), \tag{S4}$$

where Λ_{NE} is the molar conductivity (NE: Nernst–Einstein), F is the Faraday constant, RT is the gas constant times the thermodynamic temperature, v_+ and v_- are the number of cations and anions per formula unit of electrolyte, z_+ and z_- are the valences of the ions, and D_+ and D_- are the diffusion coefficients of the ions.[S10,S11] In the present study, $v_+ = 1$, $v_- = (2 \text{ or } 3)$, $z_+ = (2 \text{ or } 3)$, and $z_- = 1$. Thus, eqn (S4) is rewritten for the $\mathrm{Co^{II}(L)}_i\mathrm{(An)}_2$ ($z_+ = 2$) and $\mathrm{Co^{III}(L)}_i\mathrm{(An)}_3$ ($z_+ = 3$) species into

$$\Lambda_{\mathrm{red}} = \frac{F^2}{RT}(1 \times 2^2 \times D_{2+} + 2 \times 1^2 \times D_{-}) = \frac{F^2}{RT}(4D_{2+} + 2D_{-}) \qquad \text{(S5)}$$

and

$$\Lambda_{\mathrm{ox}} = \frac{F^2}{RT}(1 \times 3^2 \times D_{3+} + 3 \times 1^2 \times D_{-}) = \frac{F^2}{RT}(9D_{3+} + 3D_{-}), \qquad \text{(S6)}$$

respectively, where D_{2+}, D_{3+}, and D_{-} are the diffusion coefficients of $\mathrm{Co(L)}_i^{2+}$, $\mathrm{Co(L)}_i^{3+}$, and An^{-}, respectively. Because the present solutions of redox couples are a 1:1 molar mixture of "red" and "ox" species, Λ_{NE} is written as

$$\Lambda_{\mathrm{NE}} = \Lambda_{\mathrm{red}} + \Lambda_{\mathrm{ox}} = \frac{F^2}{RT}(4D_{2+} + 9D_{3+} + 5D_{-}). \qquad \text{(S7)}$$

Furthermore, the Stokes–Einstein relation for a non-slip condition is given by

$$D = \frac{k_{\mathrm{B}}}{6\pi r\eta}, \qquad \text{(S8)}$$

where k_{B} is the Boltzmann constant, r is the particle radius determined by our quantum-chemical simulations (cf. Table S1), and the constant "6π" is for perfect stick condition (vs. "4π" for perfect slip condition).[S12] By substituting eqn (S8) into eqn (S7), we obtain

$$\Lambda_{\mathrm{NE}} = \frac{F^2}{6\pi N_{\mathrm{A}}\eta}\left(\frac{4}{r_{2+}} + \frac{9}{r_{3+}} + \frac{5}{r_{\mathrm{an}}}\right), \qquad \text{(S9)}$$

which is eqn (13) in the main text.

8. Adjusted Walden plot

Figure S3 below shows the adjusted Walden plot in which the differences in ionic radii are taken into account.[S13]

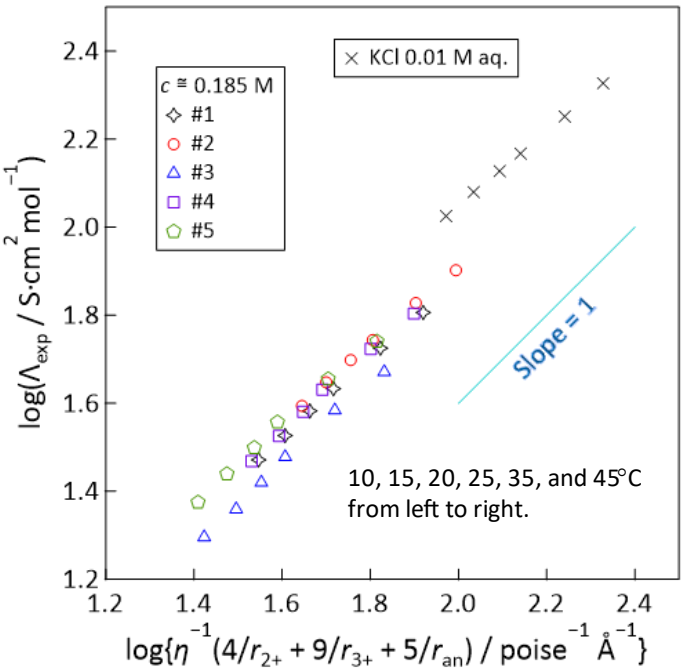

Fig. S3 The adjusted Walden plot [S13] for the electrolytes containing the redox couples #1–5 at $c \cong$ 0.185 M. In this figure, the results of 0.01 M KCl aqueous solution are also included as the reference, the datapoints of which were generated using the ionic radii of 1.38 Å and 1.81 Å for K^+ and Cl^-, respectively, as reported previously.[S14]

References

[S1] T. J. Abraham, D. R. MacFarlane and J. M. Pringle, *Energy Environ. Sci.*, 2013, **6**, 2639−2645.

[S2] J. D. Chai and M. H. Gordon, *Phys. Chem. Chem. Phys.*, 2008, **10**, 6615–6620.

[S3] M. Hamzehloueian, Y. Sarrafi and Z. Aghaei, *RSC Adv.*, 2015, **5**, 76368–76376.

[S4] Z. Zara. J. Iqbal, K. Ayub, M. Irfan, A. Mahmood, R. A. Khera and B. Eliasson, *J. Mol. Struct.*, 2017, **1149**, 282–298.

[S5] A. Bondi, *J. Phys. Chem.*, 1964, **68**, 441–451.

[S6] For example, J. A. Fay, *Introduction to Fluid Mechanics*, MIT Press, Cambridge, *MA, USA*, 1994, Chapter 10.

[S7] D. Al-Masri, M. Dupont, R. Yunis, D. R. Macfarlane, J. M. Pringle, *Electrochim. Acta*, 2018, **269**, 714–723.

[S8] Y. Ikeda, Y. Cho and Y. Murakami, *Sustain. Energy Fuels*, 2021, **5**, 5967–5974.

[S9] S. Sahami and M. J. Weaver, *J. Electroanal. Chem.*, 1981, **122**, 155–170.

[S10] "Nernst-Einstein equation" in *Oxford Reference*. URL: https://www.oxfordreference.com/view/10.1093/oi/authority.20110803100228898

[S11] K. R. Harris, *J. Phys. Chem. B*, 2019, **123**, 7014–7023.

[S12] C. Schreiner, S. Zugmann, R. Hartl and H. J. Gores, *J. Chem. Eng. Data*, 2010, **55**, 1784–1788.

[S13] D. R. MacFarlane, M. Forsyth, E. I. Izgorodina, A. P. Abbott, G. Annat and K. Fraser, *Phys. Chem. Chem. Phys.*, 2009, **11**, 4962–4967.

[S14] R. D. Shannon, *Acta Cryst. A*, 1976, **32**, 751–767.